



RESEARCH

# Discovering differential governing equations of hysteresis dynamic systems by data-driven sparse regression method

Jiawei Qian · Xiuting Sun · Jian Xu · Li Cheng

Received: 10 March 2024 / Accepted: 17 April 2024 / Published online: 9 June 2024  
© The Author(s), under exclusive licence to Springer Nature B.V. 2024

**Abstract** Hysteresis phenomenon widely exists in various metamaterials and smart actuators. Governing equations can describe and predict the static/dynamic behavior of the systems with hysteresis property. However, the hysteresis force cannot be measured nor explicitly expressed by state variables, which brings great challenge for the model reconstruction of the hysteresis systems, especially when the nonlinear restoring and damping forces also exist. In this paper, a data-driven method is proposed to reconstruct the model of the systems with both hysteresis and nonlinearity properties from dynamic information. From the proposed method, the linear, nonlinear, and hysteresis forces, can be separately reconstructed based on the data generation with incremental generation of dynamics signals under supervision. Facing to the challenge for the functional representation of hysteresis, based on an agent model, the function

library is successfully constructed. Next, for the sparsity and accuracy of the reconstruction model, the sparse regression method is generalized to identify all the nonlinear terms and coefficients. Once linear, nonlinear and hysteresis terms are figured out, the discovery of differential governing equations of hysteresis dynamic systems is completed. Three numerical examples are carried out to demonstrate the effectiveness and capability of the proposed data-driven method in the dynamic systems with different nonlinearities, dimensions and hysteresis; and the model reconstruction for Tachi-Miura polyhedron (TMP) origami structure, which possesses both hysteresis nonlinearity and geometric nonlinearity, is shown in experiments. The proposed model reconstruction method realizes the reconstruction of constitutive relation and governing equations of nonlinear hysteresis systems based on compressive sensing from dynamics, which demonstrates that great benefit of dynamic data. The model reconstruction method also provides an accurate estimation method for constitutive equation for metamaterials, robotic joint, isolation system, flexibility deployable structures, etc.

---

J. Qian · X. Sun (✉) · J. Xu  
School of Aerospace Engineering and Applied Mechanics,  
Tongji University, Shanghai, China  
e-mail: 05mech\_sunxiuting@tongji.edu.cn

X. Sun  
Key Laboratory of Ai-aided Airworthiness of Civil  
Aircraft Structures, Civil Aviation Administration of  
China, Tongji University, Shanghai, China

L. Cheng  
Department of Mechanical Engineering, The Hong Kong  
Polytechnic University, Hung Hom,  
Kowloon, Hong Kong, China

**Keywords** Model reconstruction · Hysteresis systems · Sparse regression · Data-driven method

## 1 Introduction

Hysteresis is a typical nonlinear phenomenon describing the memory-based relationship between the input and the output of the systems, where the output not only depends on the current input but also on its past history [1]. The hysteresis phenomenon is originated from magnetic, ferromagnetic and ferroelectric materials [2], and widely exists in various metamaterials [3–8] and smart actuators [9–16]. Recently, novel design of metamaterials receives a lot of attention from scholars. In particular, origami structures not only have hysteresis property [17] induced by the plastic deformation at the creases [18], but also geometric nonlinearity, which leads to various deformation mechanisms and extraordinary properties, such as negative Poisson's ratio [19, 20], multistability [21, 22], etc. In order to improve the performance of metamaterials and smart actuators, the method to obtain the accurate model for nonlinear hysteresis system is of great significance. In general, quasi-static tests could be used to reveal the hysteresis phenomena of different metamaterials and smart actuators [23–25], which could also be used to analyze the influence of different structure parameters on the hysteresis property [26, 27]. In the process of hysteresis system modeling, the memory characteristic and rate-dependent property caused by hysteresis need to be considered and accurately described. Different expressions for the hysteresis can reflect the memory characteristic, depending on the previous input and current state, and thus, the hysteresis force cannot be expanded as elementary functions of state variables; Rate-dependent property indicates the shape and size of hysteresis loop change with amplitude and frequency of external excitations, which causes the failure of quasi-static tests. Due to the memory characteristic and rate-dependent property of the input–output relationship of hysteresis systems, it is of great challenge to establish an appropriate model for hysteresis systems.

In order to give the explicit or implicit expression of nonlinear hysteresis systems, various hysteresis mathematical models have been proposed, which can be approximately divided into two categories: operator-based models [28–31] and differential-based models [32, 33]. Operator-based models use hysteresis operators to describe the hysteresis behaviors of the nonlinear systems, such as Preisach model [31],

Krasnosel'skii-Pokrovskii model [28], Prandtl-Ishlinskii model [30] and Maxwell-Slip model [29]. However, the operator-based model contains the piecewise function integral term, which is not conducive to the analysis of the system. Different from operator-based models, differential-based models use differential governing equation to characterize the hysteresis nonlinearity, such as Bouc-Wen model [33] and Duhem model [32]. The differential-based models have simple expression, which is beneficial for the identification and analysis. Among these hysteresis mathematical expressions, the Bouc-Wen model has been widely used because of its capability and versatility to describe various common hysteresis cycles [34]. Furthermore, various identification methods were developed for nonlinear hysteresis systems, which can be generally classified into two categories: non-parametric identification method and parametric identification method [35]. In non-parametric identification methods, feedforward neural network [36] and recurrent neural network [37, 38] are the most representative. Serpico et al. [39] proposed an artificial neural network scheme to realize magnetic hysteresis modeling, which was composed of a Preisach memory block and a feedforward neural network block. Based on the characteristic that recurrent neural networks can conduct time series prediction, Zakerzadeh et al. [40] used LSTM, a modified recurrent neural network, to model shape memory alloys with hysteresis and nonlinear dynamics. In parametric identification methods, the explicit forms of dynamic model are given, and the corresponding model parameters of nonlinear hysteresis systems are identified based on minimization of objective functions. Different kinds of objective functions were constructed to measure the difference between model prediction results and experimental results under different model parameters, such as the root-mean-square of displacement [34], acceleration [41], hysteretic displacement [42] etc. The optimal model parameters were obtained by minimizing the objective function using different optimization algorithm, such as Genetic algorithm [43], Particle swarm optimization algorithm [44], differential evolution algorithm [45] etc. Furthermore, multiple objective functions were used in the parameter identification process in order to improve the precision of parameter identification. Carboni et al. [46] identified the parameters of a multi-purpose rheological device by minimizing the mean square

error of the restoring force through Differential Evolutionary algorithm, and then the identified results are verified by the mean square error of the predicted displacement and the real displacement. Ortiz et al. [47] proposed a multi-objective optimization algorithm based on NSGA-II, where multiple objective functions were considered to minimize the difference in both displacement and hysteresis cycles. Recently, a novel alternating state-parameter identification method was proposed by Lin et al. [48], where two different objective functions were used in the iteratively alternating procedure to separately update the linear parameters and the nonlinear hysteresis parameters in the Bouc-Wen model, and the harmonic balance method was adopted to estimate the unmeasurable hysteresis force of the system. An additional objective function was considered in the iteratively alternating procedure to estimate the unmeasurable hysteresis force of the system [49]. Besides, nonlinear filtering could also be used to improve the accurate model parameters, such as extended Kalman filter [50, 51], unscented Kalman filter [52, 53], bootstrap filter [54] etc. However, in these previous studies, it assumes that there is no other nonlinear force except the hysteresis force during the process of identifying the hysteresis model parameters. In practical applications, not only nonlinear hysteresis forces but also other nonlinear constitutive forces such as geometric nonlinearities, exist in the engineering structures, which is always ignored in the previous parameter identification method. A model reconstruction method considering both hysteresis forces and other explicitly expressed nonlinear constitutive forces is required.

Based on the assumption that there are only a few important terms governing the dynamics of the system, Brunton et al. proposed a model reconstruction method called Sparse Identification of Nonlinear Dynamics (SINDy), which combines machine learning and sparsity regression techniques to determine the fewest terms in the dynamic governing equations required to accurately represent the data [55]. By constructing a candidate function library which contains all the possible terms, the SINDy algorithm converts the model reconstruction problem into a sparse regression problem, and the sparse regression problem is solved by sequential thresholded least-squares algorithm. Furthermore, the SINDy algorithm is extended to reconstruct dynamic models described by partial differential equations [56], which can be

used to describe the flow field and its dynamics [57–59]. Then, Messenger et al. [60, 61] proposed a weak SINDy algorithm based on the weak formulation of the differential equation to avoid approximation of pointwise derivatives and improve the robustness to noise. The weak SINDy was utilized to reconstruct the mean-field equations of interacting particle systems [62]. In order to reconstruct the dynamic model of a multistable dynamic system, we had proposed a generalized data-driven reconstruction method based on data assembly principle and sparsification parameter determination to construct ergodic dataset and resolve the difficulty on the determination of sparsification parameter [63]. Furthermore, the generalized data-driven reconstruction method was extended to non-autonomous nonlinear systems with multiple attractors, where the accurate description is obtained under the least volume of test data set [64]. The main idea to deal with external inputs is that the external inputs of the system as treated as measurable variable in the function library matrix. In summary, when applying the SINDy algorithm, it is required that the state variables can be measured directly or obtained by taking derivative or integral of other state variables, and all the terms in the governing equations can be expressed by the elementary functions of state variables. However, for nonlinear hysteresis systems, the hysteresis force can neither be directly measured nor be obtained by taking derivative or integral of state variables. Besides, hysteresis forces cannot be expressed by the elementary functions of state variables, which poses a great challenge to building an appropriate library. Therefore, for the identification and description of the nonlinear systems with hysteresis property, the following challenges are faced in the model reconstruction: (a) How to extract information about hysteresis force during data generation; (b) How to build an appropriate library function matrix for system containing both nonlinearity and hysteresis.

In this paper, faced to the challenges above on the reconstruction of the constitutive relation and governing equations of hysteresis systems, a data-driven model reconstruction method is proposed. In the supervised data generation, the training data is generated with supervision, and the linearity and nonlinearity of the system are decoupled in order to reconstruct the nonlinear forces and hysteresis force. Then, the agent model of the original hysteresis system is established, and the nonlinear function

library is constructed based on the agent model. By three numerical examples and one experiment, the effectiveness and capability of the proposed data-driven method is demonstrated. In the experiment, an origami structure is given as the verification case of the proposed method. In the origami structure, the nonlinearity comes from two aspects: the geometric nonlinearity brought by the nonlinear geometric arrangement with creases and the constitutive nonlinearity and hysteretic nonlinearity caused by non-rigid facets. Thus, the novelties of this paper are as follow. Firstly, the form of geometric nonlinearity, hysteresis nonlinearity and constitutive nonlinearity are separated and explicated in the reconstruction model. Secondly, it gives the exact expression and prediction of the hysteresis nonlinear constitutive of different structures and materials for different loading amplitude utilizing dynamic information. The rest of the paper is organized as follows: Sect. 2 introduces the procedure of the data-driven reconstruction method, including multistep excitation step, nonlinear function library construction step and nonlinear parameter solving step. To demonstrate the effectiveness and

capability of the proposed data-driven reconstruction method, three numerical examples are carried out in Sect. 3. After that, the data-driven model reconstruction method is used to obtain the governing equations of a TMP origami structure in Sect. 4. Finally, the conclusions are presented in Sect. 5.

### 2 Model reconstruction method

For hysteresis systems, it is of importance to obtain accurate representation of the constitutive relations to serve for the analysis and prediction of statics and dynamic behaviors. Figure 1 shows different experimental approaches to obtain the constitutive relations. Usually, quasi-static tension and compression tests, as shown in Fig. 1 a, are utilized to obtain the constitutive relation of the materials or structures by a test specimen. In the quasi-static tests, since the hysteresis property depends on different loading velocity, the constitutive relations of hysteresis cannot be reconstructed from the quasi-static tests, due to the lack of dynamic response signals. On the contrary, for

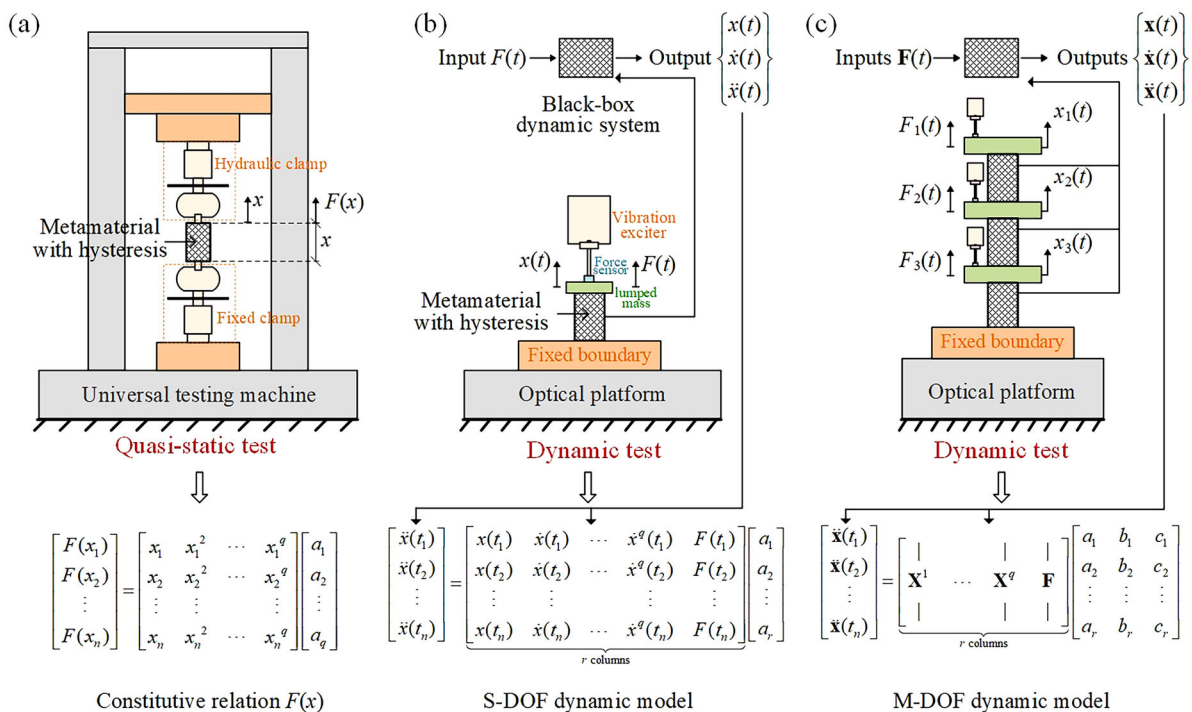


**Fig. 1** Different approaches to obtain constitutive relation of metamaterials with hysteresis and nonlinear properties. **a** Quasi-static test by single tension and the constitutive relation

reconstruction process from the test data; **b** Dynamic test for homogeneous metamaterial with hysteresis in one direction; **c** Dynamic test for inhomogeneous metamaterial with hysteresis

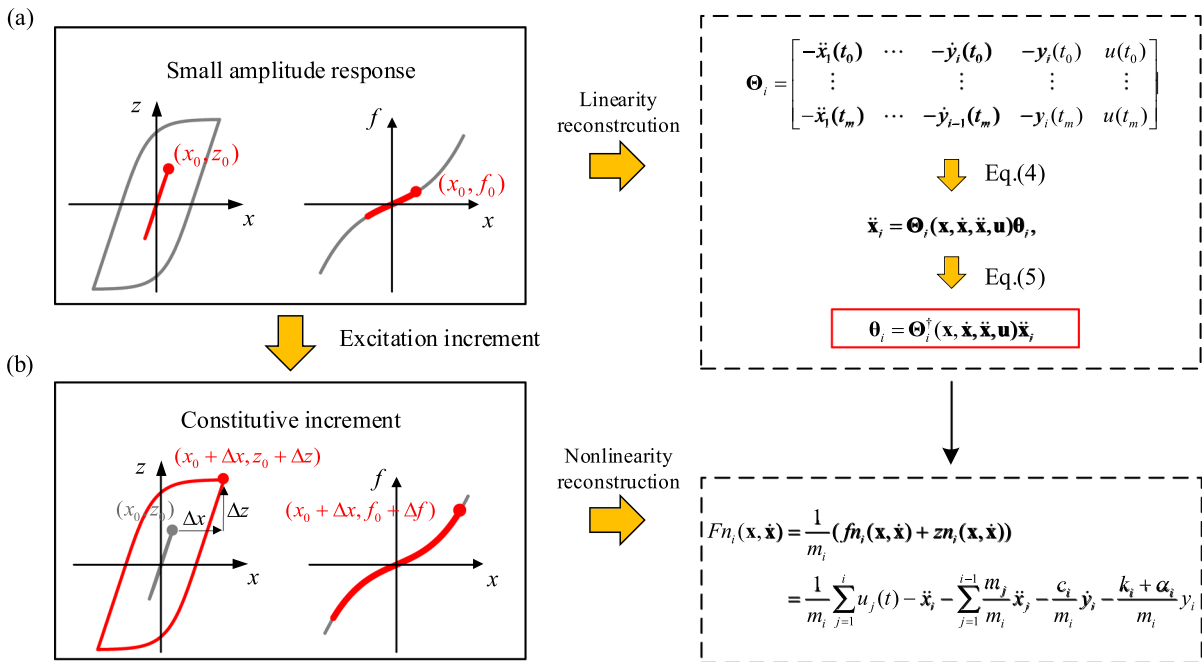


**Fig. 2** Computational framework of supervised data generation for model reconstruction. **a** Parameter identification for linearization constitutive relation; **b** Nonlinear constitutive relation reconstruction by increment of dynamic behaviors

dynamic data, the constitutive relation between hysteresis force and deformation can be perceived, since the dynamic information of velocity and acceleration are included in the data. As the dynamic experiment shown in Fig. 1b, assuming the homogeneity in the main direction, a dynamical input  $F(t)$  is given, and the responses signals  $\mathbf{x}(t), \dot{\mathbf{x}}(t), \ddot{\mathbf{x}}(t)$  can be estimated. Furthermore, when the material properties are not uniform, as the experiment shown in Fig. 1c, for dynamic input  $\mathbf{F}(t)$ , the differential governing equations of the system constitute M-DOF nonlinear hysteresis systems. For the responses  $\mathbf{x}(t), \dot{\mathbf{x}}(t), \ddot{\mathbf{x}}(t)$  estimated for the reconstruction, the governing equation of nonlinear hysteresis systems is described as

$$\mathbf{M}\ddot{\mathbf{x}} = \mathbf{f}(\mathbf{x}, \dot{\mathbf{x}}) + \mathbf{z}(\mathbf{x}, \dot{\mathbf{x}}) + \mathbf{u} \tag{1}$$

where  $\mathbf{x} = [x_1 \ x_2 \ \cdots \ x_n]^T$  denotes the displacements of measurement points in the system, vector  $\mathbf{u}$  represents external excitation;  $\mathbf{f}(\mathbf{x}, \dot{\mathbf{x}})$  contains restoring and damping forces, both can be expressed by elementary functions of state variables; while  $\mathbf{z}(\mathbf{x}, \dot{\mathbf{x}})$  represents the hysteresis force which cannot be expressed by elementary functions of state variables. The main difficulty of model reconstruction of nonlinear hysteresis systems is that hysteresis force can

neither be measured directly nor expressed by elementary functions of other state variables. Therefore, in this study, we establish a data-driven method to reconstruct the governing equations of nonlinear systems with hysteresis and nonlinearity from dynamic information. Firstly, in order to separately reconstruct the linear, nonlinear, and hysteresis forces, data are generated based on the incremental generation of dynamics under supervision. Then, by substituting hysteresis force with nonlinear force, an agent model for the original hysteresis system is established, and the nonlinear constitutive function library matrix is constructed based on the agent model. At last, all the terms including linear, nonlinear and hysteresis are figured out by the generalized sparse regression technique. In summary, the proposed model reconstruction process contains three steps: Step 1, Supervised data generation; Step 2, Nonlinear constitutive function library construction; Step 3, Nonlinear parameters regression.

### 2.1 Step 1: supervised data generation

The effect of nonlinearity and hysteresis depends on the magnitude of response amplitude, which is the

typical characteristics for nonlinear systems. Initially, when the amplitude of responses is very small, the linearization part of a dynamic system plays the dominant role. With the incrementation of the response amplitudes, larger amplitude of responses demonstrates more obvious effectiveness of nonlinearity and hysteresis properties on dynamic behaviors. Thus, through the perception of the magnitudes of response amplitude, data is generated under supervision for reconstruction of linearity and nonlinearity. Therefore, the computational framework of supervised data generation in the model reconstruction method is shown in Fig. 2.

First, the linearization constitutive relation of the system can be reconstructed under small amplitude responses. As shown in Fig. 2a, since amplitudes of the responses are small, nonlinearity and hysteresis have little effect. The linearization equation of Eq. (1) is written as

$$\ddot{x}_i + \sum_{j=1}^{i-1} \frac{m_j}{m_i} \ddot{x}_j + \frac{c_i}{m_i} \dot{y}_i + \frac{k_i + \alpha_i}{m_i} y_i = \frac{1}{m_i} \sum_{j=1}^i u_j(t), i = 1, \dots, n, \quad (2)$$

where

$$\mathbf{y} = [y_1 \ y_2 \ \cdots \ y_{n-1} \ y_n]^T \\ = [x_1 - x_2 \ x_2 - x_3 \ \cdots \ x_{n-1} - x_n \ x_n]^T. \quad (3)$$

Then, as Fig. 2a, after assembly of dynamic response data for small amplitudes, the following regression problem for linearization system can be easily constructed as

$$\ddot{\mathbf{x}}_i = \mathbf{\Theta}_i(\mathbf{x}, \dot{\mathbf{x}}, \ddot{\mathbf{x}}, \mathbf{u}) \boldsymbol{\theta}_i, \quad (4)$$

where  $\boldsymbol{\theta}_i$  is the linearization parameters of the nonlinear hysteresis system,  $\mathbf{\Theta}_i(\mathbf{x}, \dot{\mathbf{x}}, \ddot{\mathbf{x}}, \mathbf{u})$  is the corresponding function library matrix (see details in Appendix 1). Here, it is assumed that the external excitations  $\mathbf{u}$  could be directly measured or indirectly approximated, and the external inputs of the system are considered as library functions in the function library matrix. Thus, in this way, we can consider the case where the system is non-autonomous. By solving the least squares solution of the contradictory equations Eq. (4), the linear parameters of the nonlinear hysteresis system can be obtained as

$$\boldsymbol{\theta}_i = \mathbf{\Theta}_i^\dagger(\mathbf{x}, \dot{\mathbf{x}}, \ddot{\mathbf{x}}, \mathbf{u}) \ddot{\mathbf{x}}_i, \quad (5)$$

where  $\mathbf{\Theta}_i^\dagger(\mathbf{x}, \dot{\mathbf{x}}, \ddot{\mathbf{x}}, \mathbf{u})$  represents the Moore–Penrose inverse of the linear function library matrix  $\mathbf{\Theta}_i(\mathbf{x}, \dot{\mathbf{x}}, \ddot{\mathbf{x}}, \mathbf{u})$ . Whereas as shown in Fig. 2b, when the amplitudes of response increase, the effect of nonlinearity and hysteresis increases. The governing equations of the system Eq. (1) can be rewritten as

$$\ddot{x}_i + \sum_{j=1}^{i-1} \frac{m_j}{m_i} \ddot{x}_j + \frac{c_i}{m_i} \dot{y}_i + \frac{k_i + \alpha_i}{m_i} y_i + \frac{1}{m_i} f n_i + \frac{1}{m_i} z n_i \\ = \frac{1}{m_i} \sum_{j=1}^i u_j(t), i = 1, \dots, n, \quad (6)$$

where  $f n_i$  represents the nonlinear part of restoring and damping forces, expressed by the elementary functions of state variables;  $z n_i$  represents the nonlinear part of hysteresis force. Based on Eq. (6), the nonlinear force is given as

$$F n_i(\mathbf{x}, \dot{\mathbf{x}}) = \frac{1}{m_i} (f n_i(\mathbf{x}, \dot{\mathbf{x}}) + z n_i(\mathbf{x}, \dot{\mathbf{x}})) \\ = \frac{1}{m_i} \sum_{j=1}^i u_j(t) - \ddot{x}_i - \sum_{j=1}^{i-1} \frac{m_j}{m_i} \ddot{x}_j - \frac{c_i}{m_i} \dot{y}_i \\ - \frac{k_i + \alpha_i}{m_i} y_i, i = 1, \dots, n. \quad (7)$$

So far, both linearity and nonlinearity are reconstructed. In Eq. (7), the nonlinear force  $F n_i(\mathbf{x}, \dot{\mathbf{x}})$  contains both the nonlinear restoring force and damping forces  $f n_i(\mathbf{x}, \dot{\mathbf{x}})$ , which can be expressed by the elementary functions of other state variables; while the nonlinear part of the hysteresis force  $z n_i(\mathbf{x}, \dot{\mathbf{x}})$  cannot be expressed by the elementary functions of other state variables. This results in the inability to build appropriate function library during the reconstruction of nonlinear forces, and thus, it requires the technique for function library determination for the hysteresis system, called Step 2 in the following illustration.

## 2.2 Step 2: Nonlinear constitutive function library construction

In order to solve the construction of appropriate function library for hysteresis system, the nonlinear force  $F n_i(\mathbf{x}, \dot{\mathbf{x}})$ , instead of hysteresis force  $z(\mathbf{x}, \dot{\mathbf{x}})$ , is

selected to establish the agent model. To start with, the Bouc-Wen model is adopted to describe the hysteresis force  $z(\mathbf{x}, \dot{\mathbf{x}})$  as

$$\dot{z}_i(\mathbf{x}, \dot{\mathbf{x}}) = \alpha_i \dot{y}_i - \gamma_i |\dot{y}_i| z_i - \delta_i \dot{y}_i |z_i|, i = 1, 2, \dots, n. \tag{8}$$

The parameters  $\alpha_i, \gamma_i, \delta_i$  are the hysteresis coefficients, determining the size and shape of hysteresis loops. In Eq. (8), the term  $\alpha_i \dot{y}_i$  has the same effect as linear restoring force, which is included in the reconstruction of linearity instead of nonlinearity. Thus, the nonlinear part of hysteresis force  $zn_i(\mathbf{x}, \dot{\mathbf{x}})$  can be expressed as

$$zn_i = z_i - \alpha_i y_i, i = 1, 2, \dots, n. \tag{9}$$

Substitute hysteresis force  $z(\mathbf{x}, \dot{\mathbf{x}})$  by the nonlinear force  $Fn_i(\mathbf{x}, \dot{\mathbf{x}})$ , the agent model can be given as

$$\begin{aligned} \dot{F}n_i(\mathbf{x}, \dot{\mathbf{x}}) &= \frac{1}{m_i} (\dot{f}n_i(\mathbf{x}, \dot{\mathbf{x}}) + \dot{z}n_i(\mathbf{x}, \dot{\mathbf{x}})) \\ &= \frac{1}{m_i} \dot{f}n_i - \frac{\gamma_i}{m_i} |\dot{y}_i| (zn_i + \alpha_i y_i) \\ &\quad - \frac{\delta_i}{m_i} \dot{y}_i |zn_i + \alpha_i y_i|, i \\ &= 1, \dots, n. \end{aligned} \tag{10}$$

In Eq. (10),  $|zn_i + \alpha_i y_i|$  is the absolute value of hysteresis force  $z_i(x, \dot{x})$ , which indicates that the absolute value sign can be eliminated by identifying the sign of hysteresis force. Equation (10) is used as the agent model for constructing nonlinear constitutive function library. Thus, the supervision process of data based on the sign of the hysteresis force is proposed as Fig. 3, which helps the determination of constitutive function library.

In Fig. 3a, in the hysteresis loop, points A and C denote the zero displacement while points B and D denote the maximum displacement. For the interval AB in the hysteresis loop, the sign of the hysteresis force is positive, while for the interval CD, the sign of the hysteresis force is negative. Therefore, when the system is in the interval AB or interval CD, the agent model of Eq. (10) can be rewritten as

$$\begin{aligned} \dot{F}n_i(\mathbf{x}, \dot{\mathbf{x}}) &= \frac{1}{m_i} \dot{f}n_i \pm \lambda_i \dot{y}_i (Fn_i - \frac{1}{m_i} \dot{f}n_i + \frac{\alpha_i}{m_i} y_i), i \\ &= 1, \dots, n, \end{aligned} \tag{11}$$

where  $\lambda_i = \gamma_i + \delta_i$ . The time history data in hysteresis loop in Fig. 3b are utilized to find out the conditions that the dynamic signals of the agent system are in the

interval AB or CD. From Fig. 3b, the system is in the interval AB if and only if  $y_i \geq 0, \dot{y}_i \geq 0$ , and in the interval CD if and only if  $y_i \leq 0, \dot{y}_i \leq 0$ . Based on the data information and the analysis above, the data clustering and nonlinear constitutive function library construction process are shown in Fig. 3c, with the following two techniques. First, the collected data matrix  $\mathbf{X}$  is converted to data matrix  $\mathbf{Y}$  by a linear transformation to converts absolute coordinates to relative coordinates. Then, supervised data clustering is performed on data matrix  $\mathbf{Y}$  through a clustering element. The clustering element puts the input data into the kernel function  $h(y_i, \dot{y}_i)$ , and clustering the data through the output value of the kernel function. The kernel function  $h(y_i, \dot{y}_i)$  is defined as

$$h(y_i, \dot{y}_i) = \text{sgn}(\text{sgn}(y_i) + \text{sgn}(\dot{y}_i)), \tag{12}$$

where  $\text{sgn}(\cdot)$  stands for sign function. When the output of kernel function  $h(y_i, \dot{y}_i)$  is 1, the dynamic signals are in the interval AB; When the output of kernel function  $h(y_i, \dot{y}_i)$  is -1, the dynamic signals are in the interval CD; When the output of kernel function  $h(y_i, \dot{y}_i)$  is 0, the dynamic signals are in the interval BC or DA. According to Eq. (11), we assume that the nonlinear force  $\dot{f}n_i(\mathbf{x}, \dot{\mathbf{x}})$  can be expressed by high-order polynomial functions of  $\mathbf{x}, \dot{\mathbf{x}}$  as

$$\dot{f}n_i(\mathbf{x}, \dot{\mathbf{x}}) = m_i (a_{i1} y_i^2 + a_{i2} y_i \dot{y}_i + a_{i3} \dot{y}_i^2 + a_{i4} y_i^3 + \dots). \tag{13}$$

Then, the derivation function  $\dot{f}n_i(\mathbf{x}, \dot{\mathbf{x}})$  is expressed as

$$\begin{aligned} \dot{f}n_i(\mathbf{x}, \dot{\mathbf{x}}) &= m_i (a_{i1} (2y_i \dot{y}_i) + a_{i2} (\dot{y}_i^2 + y_i \ddot{y}_i) + a_{i3} (2\dot{y}_i \ddot{y}_i) \\ &\quad + a_{i4} (3y_i^2 \dot{y}_i) + \dots). \end{aligned} \tag{14}$$

Therefore, the nonlinear constitutive function library matrix is constructed as

$$\Theta_{\mathbf{n}_i}(y_i, \dot{y}_i, \ddot{y}_i, \mathbf{F}\mathbf{n}_i) = \begin{bmatrix} | & | & | & | & | & | & | & | & | \\ \overline{\mathbf{Y}}_i^2 \odot \mathbf{Y}_i^2 & \dots & \overline{\mathbf{Y}}_i^q \odot \mathbf{Y}_i^q & \dot{\mathbf{Y}}_i^2 & \dots & \dot{\mathbf{Y}}_i^q & \mathbf{y}_i \odot \dot{\mathbf{y}}_i & -\mathbf{y}_i \odot \mathbf{F}\mathbf{n}_i & \\ | & | & | & | & | & | & | & | & | \end{bmatrix}, \tag{15}$$

where  $q$  is the highest order of polynomial function  $\dot{f}n_i(\mathbf{x}, \dot{\mathbf{x}})$ , matrices  $\overline{\mathbf{Y}}_i^m, \mathbf{Y}_i^m, \dot{\mathbf{Y}}_i^m$  are

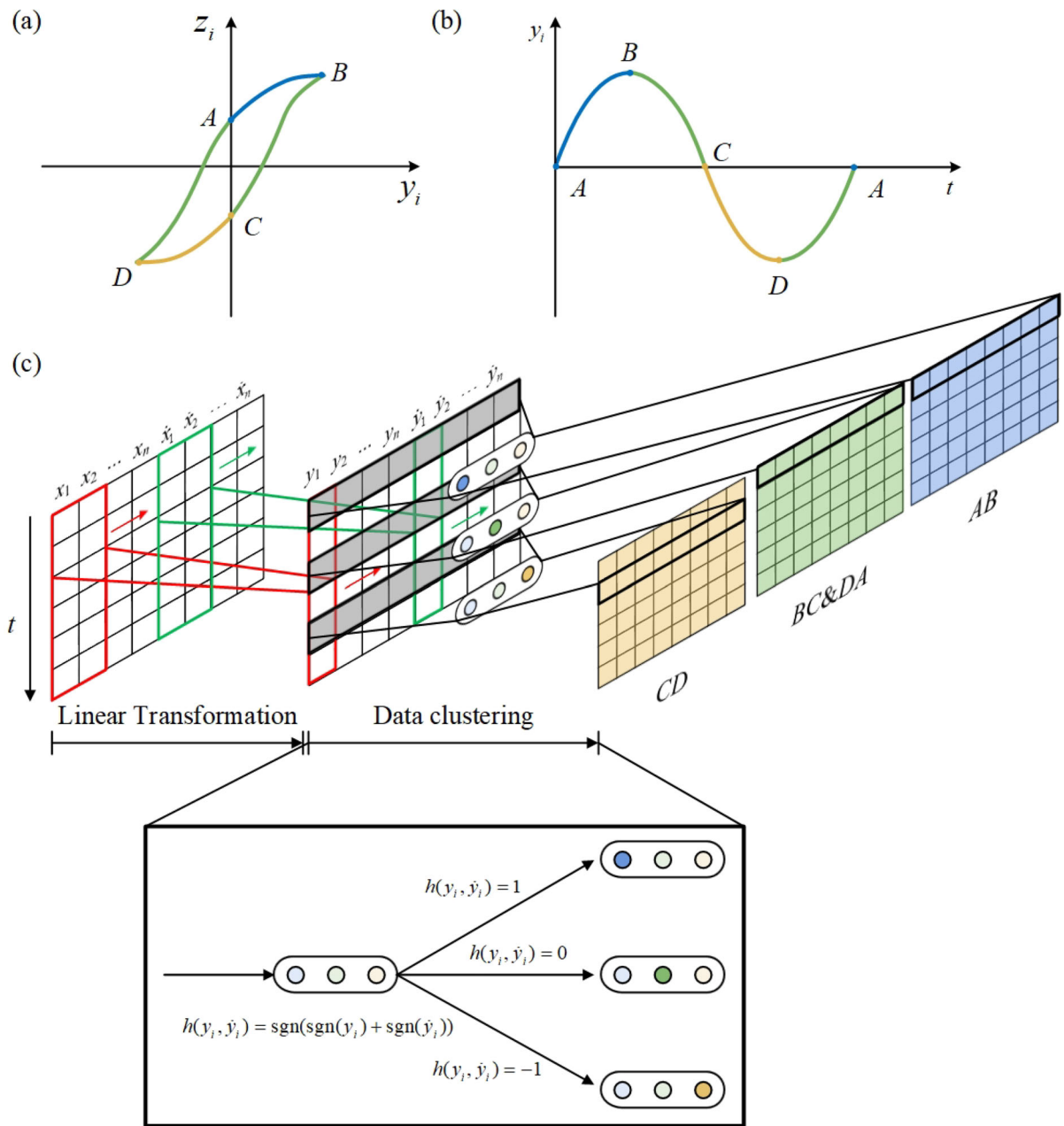


**Fig. 3** The supervision and categorization process of data. **a** Different phases in the hysteresis loop; **b** Time history corresponding to the different phases in hysteresis loop; **c** Schematic diagram of the proposed data collection and assembly process with supervision

$$\bar{\mathbf{Y}}_i^m = \left[ \underbrace{\dot{y}_i \ \dots \ \dot{y}_i}_{m+1 \text{ columns}} \right], \quad (16)$$

$$\mathbf{Y}_i^m = \left[ \begin{array}{c|c|c|c|c} | & | & | & | & | \\ y_i^m & y_i^{m-1}\dot{y}_i & y_i^{m-2}\dot{y}_i^2 & \dots & \dot{y}_i^m \\ | & | & | & | & | \end{array} \right], \quad (17)$$

$$\dot{\mathbf{Y}}_i^m = \left[ \begin{array}{c|c|c|c} \frac{d(y_i^{m-1}\dot{y}_i)}{dt} & \frac{d(y_i^{m-2}\dot{y}_i^2)}{dt} & \dots & \frac{d(y_i^m)}{dt} \end{array} \right]. \tag{18}$$

After the data clustering process, the nonlinear constitutive function library  $\Theta_{\mathbf{n}_i}$  can be constructed by dynamic signals in the interval  $AB$  or  $CD$ . Thus, the expression of function library for the hysteresis and nonlinear systems is solved by agent model.

### 2.3 Step3: Parameters regression process

After the definition of function library as Eq. (15) based on the agent model, efficient regression algorithm provides successful interpretability reconstruction of the constitutive relation with nonlinearity and hysteresis. Substituting Eq. (13) and Eq. (14) into Eq. (11), the regression problem can be constructed as

$$\dot{\mathbf{F}}\mathbf{n}_i(\mathbf{x}, \dot{\mathbf{x}}) = \Theta_{\mathbf{n}_i}(\mathbf{y}_i, \dot{\mathbf{y}}_i; \mathbf{f}_i, \mathbf{F}\mathbf{n}_i)\theta_{\mathbf{n}_i}, \tag{19}$$

where  $\theta_{\mathbf{n}_i}$  represents the nonlinear coefficients for the library functions. Specifically, the form of  $\theta_{\mathbf{n}_i}$  is written as

$$\theta_{\mathbf{n}_i} = \left[ \xi_{i2} \quad \dots \quad \xi_{iq} \quad \psi_{i2} \quad \dots \quad \psi_{iq} \quad 2a_{i1} - \frac{\lambda_i \alpha_i}{m_i} \quad \lambda_i \right]^T, \tag{20}$$

where

$$\xi_{ij} = \begin{cases} [\lambda_i a_{ip_j} + (j+1)a_{ip_{j+1}} \quad \lambda_i a_{i(p_j+1)} \quad \dots \quad \lambda_i a_{i(p_{j+1}-1)}] = [\lambda_i a_{ip_j} + (j+1)a_{ip_{j+1}} \quad \bar{\xi}_{ij}], j = 2, \dots, q-1, \\ [\lambda_i a_{ip_j} \quad \lambda_i a_{i(p_j+1)} \quad \dots \quad \lambda_i a_{i(p_{j+1}-1)}] = [\lambda_i a_{ip_j} \quad \bar{\xi}_{ij}], j = q, \end{cases} \tag{21}$$

$$\Psi_{ij} = [a_{i(p_j+1)} \quad a_{i(p_j+2)} \quad \dots \quad a_{i(p_{j+1}-1)}], \tag{22}$$

$$p_j = \frac{j(j+1)-4}{2}, j = 2, 3, \dots, q. \tag{23}$$

In order to figure out all nonlinear terms, the sparse regression process is adopted. Figure 4 shows the

proposed parameter regression process, after the supervised data generation (Step 1) and nonlinear constitutive function library construction (Step 2). The regression utilizes sparse regression technique, which takes both accuracy and sparsity of the model into consideration. Next, the proposed regression process is introduced.

As shown in Fig. 4, from the beginning of this step, all the nonlinear coefficients  $\theta_{\mathbf{n}_i}$  are solved using sequential thresholded least-squares method and sparsification parameter determination technique(Qian, et al., 2023). All the parameters are divided into three categories:  $\mathbf{D} = [\mathbf{a}_{i(p_1+1)} \quad \dots \quad \mathbf{a}_{i(p_q-1)}]$  corresponds to the nonlinear damping terms;  $\mathbf{R} = [\boldsymbol{\alpha}_i \quad \mathbf{a}_{ip_1} \quad \dots \quad \mathbf{a}_{ip_q}]$  corresponds to the nonlinear restoring terms;  $\mathbf{H} = [\boldsymbol{\gamma}_i \quad \boldsymbol{\delta}_i]$  corresponds to the hysteresis terms. First, nonlinear damping terms  $\mathbf{D}$  are directly taken from  $\Psi_{ij}$  as Eq. (22). Next, the value of  $\lambda_i$  is determined by solving the following optimization problem as

$$\lambda_i = \arg \min_{\lambda_i} \sum_{j=2}^q \left( \|\bar{\xi}_{ij} - \lambda_i \Psi_{ij}\|^2 \right). \tag{24}$$

After that, the nonlinear restoring terms  $\mathbf{R}$  can be solved by using the first element in  $\Psi_{ij}$  as Eq. (21). Finally, it can be seen from Eqs. (11) and (12) that the hysteresis terms  $\mathbf{H}$  cannot be separated when time history data in the interval  $AB$  or  $CD$  is used. The remaining time history data need to be utilized to solve

for the hysteresis terms  $\mathbf{H}$ . According to Eq. (10), the hysteresis terms  $\mathbf{H}$  can be obtained as

$$\delta_i = \mathbf{1}^\dagger \mathbf{r}, \tag{25}$$

$$\gamma_i = \lambda_i - \delta_i,$$

where

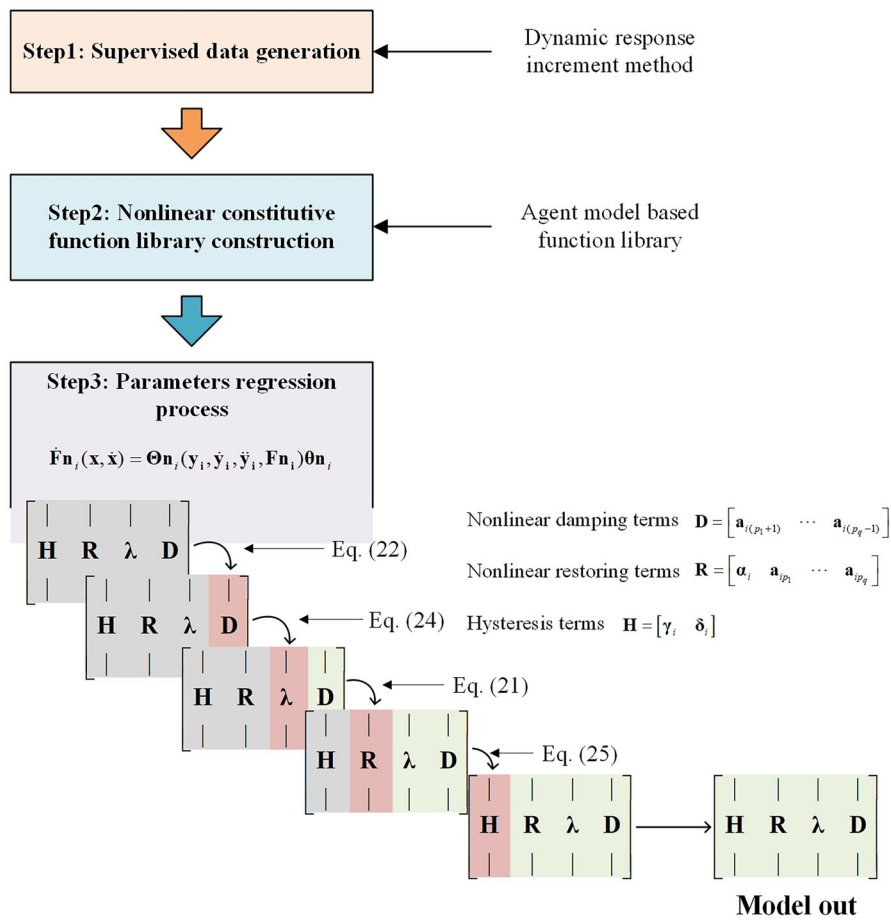


**Fig. 4** The parameters regression process

$$\mathbf{l} = \dot{\mathbf{F}}\mathbf{n}_i - \frac{1}{m_i} \dot{\mathbf{f}}\mathbf{n}_i + \frac{\lambda_i}{m_i} |\dot{\mathbf{y}}_i| \odot (\mathbf{F}\mathbf{n}_i - \frac{1}{m_i} \mathbf{f}\mathbf{n}_i + \alpha_i \mathbf{y}_i),$$

$$\mathbf{r} = -\frac{1}{m_i} (\dot{\mathbf{y}}_i \odot |\mathbf{z}\mathbf{n}_i + \alpha_i \mathbf{y}_i| - |\dot{\mathbf{y}}_i| \odot (\mathbf{z}\mathbf{n}_i + \alpha_i \mathbf{y}_i)).$$

(26)

Once  $a_{i1}, a_{i2}, \dots, a_{ip_q}, \alpha_i, \gamma_i, \delta_i$  are determined, the discovery of differential governing equations of the nonlinear and hysteresis systems is completed.

### 3 Numerical examples

In this section, three numerical examples are utilized to verify the effectiveness and applicability of the proposed data-driven model reconstruction method. The first example is a single-degree-of-freedom

(S-DOF) hysteresis system with nonlinear damping force. In this example, the process of the data-driven model reconstruction method is explained in detail, and the effectiveness of the method is verified. The second example is a nonlinear vibration isolation system with magneto-rheological damper to show that different hysteresis expressions can be reconstructed by the agent model. Different from the first example, the expression of hysteresis force is not consistent with that in Eq. (8), and the nonlinear restoring force of the system is taken into account. The third example is a multiple-degrees-of-freedom (M-DOF) nonlinear hysteresis system. Through this example, the applicability of the proposed method to nonlinear hysteresis systems with multiple degrees of freedom is demonstrated.



away from resonance is first applied to hysteresis system to generate small amplitude response. The frequency range of the sweep signal is 10–20 Hz, and the sweep speed is 0.5 Hz/s. The small amplitude response data are used to identify the linear parameters  $\theta_l$  of the hysteresis system by least squares solution (Eq. (5)). A sweep force excitation with another frequency range is then applied to hysteresis system to generate large amplitude response, whose frequency range is 50–90 Hz, and sweep speed is 2 Hz/s. The large-amplitude responses containing nonlinearity and hysteresis effectiveness are captured. In Step 2 Nonlinear constitutive function library construction: the large amplitude response data are clustered by the output of the kernel function. In Fig. 5a, the data in the interval AB of the hysteresis loop are represented by red points while other data are represented by blue points. After the data clustering process, the nonlinear constitutive function library is constructed using the data in the interval AB according to Eqs. (15–18). Here, the candidate functions for the nonlinear restoring forces and damping forces are chosen as polynomial functions up to fifth order, the corresponding library functions in the nonlinear constitutive function library matrix  $\Theta n_i$  can be obtained by Eqs. (15–18). The details of the nonlinear constitutive function library matrix  $\Theta n_i$  and the corresponding nonlinear coefficients can be seen in Appendix 2. In Step 3 Parameters regression process: the nonlinear coefficients (see details in Appendix 2) are first solved using

sequential thresholded least-squares method. Then, the model parameters are solved step by step as shown in Fig. 5a. After all the model parameters are obtained, the differential governing equations of hysteresis dynamic system is discovered.

The results are shown in Fig. 5b, where the time history responses and hysteresis loop are compared. It can be observed from Fig. 5 that the proposed data-driven method successfully predicts the time history responses of the hysteresis system, and the hysteresis force can be accurately reconstructed, which verifies the effectiveness of the proposed data-driven method. This indicates that our data-driven method has the capability to simultaneously reconstruct explicitly expressed nonlinear forces and hysteresis forces.

### 3.2 The model reconstruction of nonlinear hysteresis system by different expression

In the previous example, the Bouc-Wen model (Eq. 8) is used to describe the hysteresis force in the S-DOF degradation model. However, different hysteresis models may be encountered in application. In this example, a nonlinear vibration isolator with magnetorheological damper (Dutta and Chakraborty, 2014) is considered. The schematic diagram of the vibration isolator and the governing equations are shown in Fig. 6. It should be pointed out that the hysteresis model is different from that described by Eq. (8). In

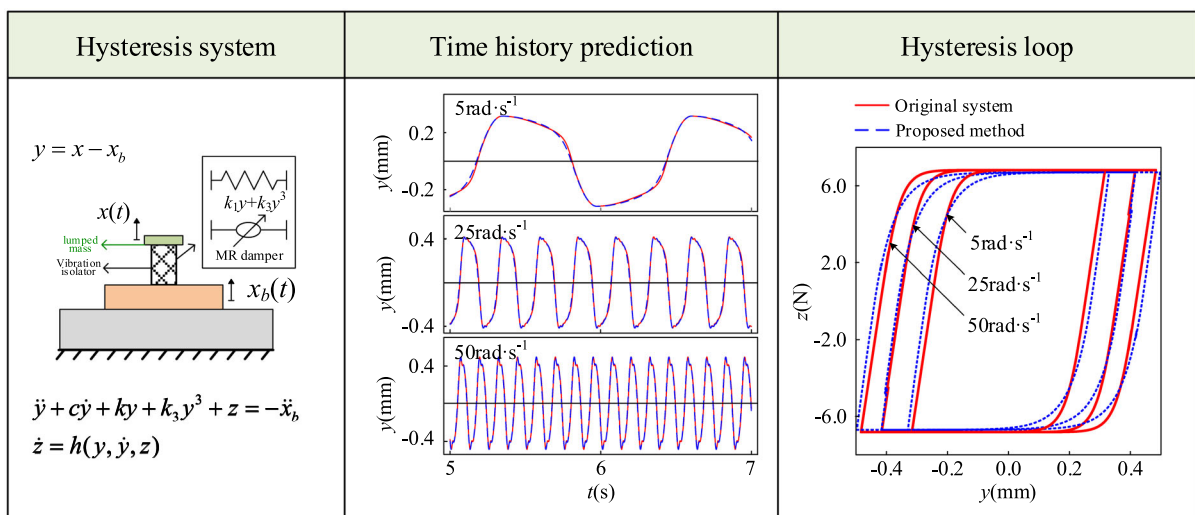


Fig. 6 Model reconstruction results for nonlinear hysteresis system by different expression

this example, the ability to reconstruct hysteresis loops described by different models is tested.

According to the proposed data-driven method, the model reconstruction of the nonlinear vibration isolator with magnetorheological damper is carried out. The discrete time history data of excitation and state variables is collected with a prescribed sampling frequency of 1000 Hz. Gaussian white noise with an 80 dB signal-to-noise ratio is added to the collected data to simulate the measurement error. The candidate functions for the nonlinear restoring forces and damping forces are chosen as polynomial functions up to fifth order, the corresponding library functions in the nonlinear constitutive function library matrix  $\Theta_{n_i}$  can be obtained by Eqs. (15–18). The reconstruction result is shown in Fig. 6, where time history response and hysteresis loop under sinusoidal excitations with different frequency and amplitude are compared. The results show a good agreement in not only time history response but also hysteresis loop. This indicates that our data-driven method is able to reconstruct hysteresis loop governed by different kinds of equations, which could contribute to the reconstruction of nonlinear constitutive relations and hysteresis loops of real systems.

### 3.3 Multi-layers nonlinear hysteresis system

#### 3.3.1 Two-layers nonlinear hysteresis system

To demonstrate the capability of the proposed data-driven method to reconstruct the dynamic model of M-DOF hysteresis systems, a two-layer nonlinear hysteresis system is studied here. The two-layer nonlinear hysteresis system consists of two masses connected by linear springs and viscous dashpots, as shown in Fig. 7. The sampling is with a frequency 1000 Hz and a duration of 20 s. The simulated signal is corrupted with white Gaussian noise with a signal-to-noise ratio of 80 dB. The candidate functions for the nonlinear restoring forces and damping forces are chosen as polynomial functions up to fifth order, the corresponding library functions in the nonlinear constitutive function library matrix  $\Theta_{n_i}$  can be obtained by Eqs. (15–18). With the proposed data-driven method, the model reconstruction results are shown in the third row of Fig. 7.

The data-driven method successfully discovers the governing equations of the two-layer nonlinear hysteresis system, and the model parameters have good precision, which results in a good agreement in the time history response and hysteresis loop. Different from the above two examples in which only one variable in the governing equations is unmeasurable, a two degrees of freedom problem shows the feasibility

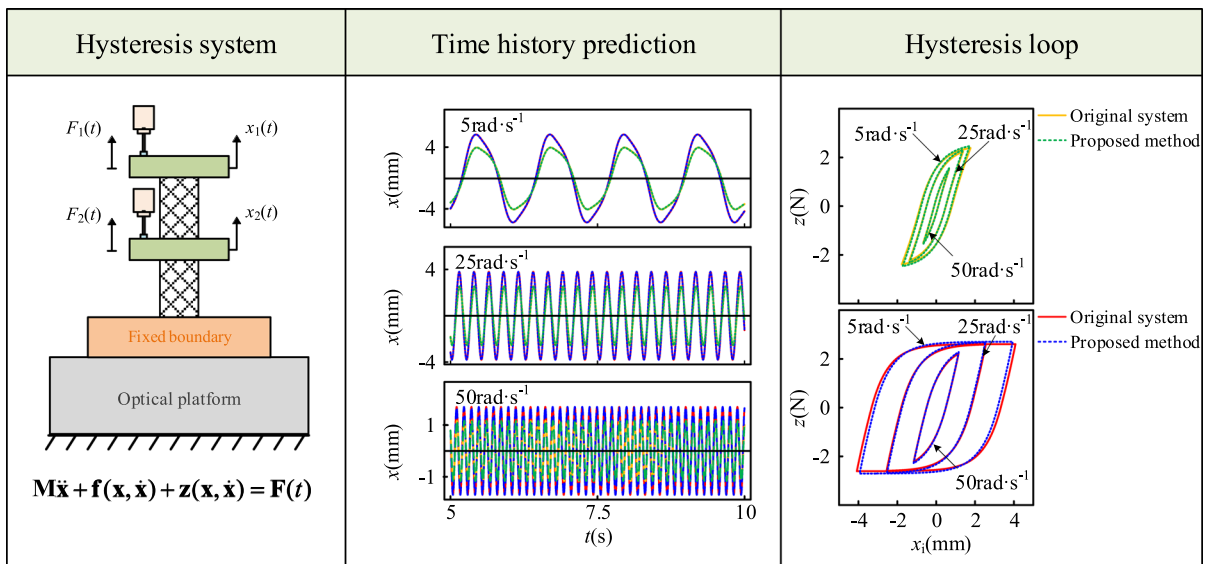
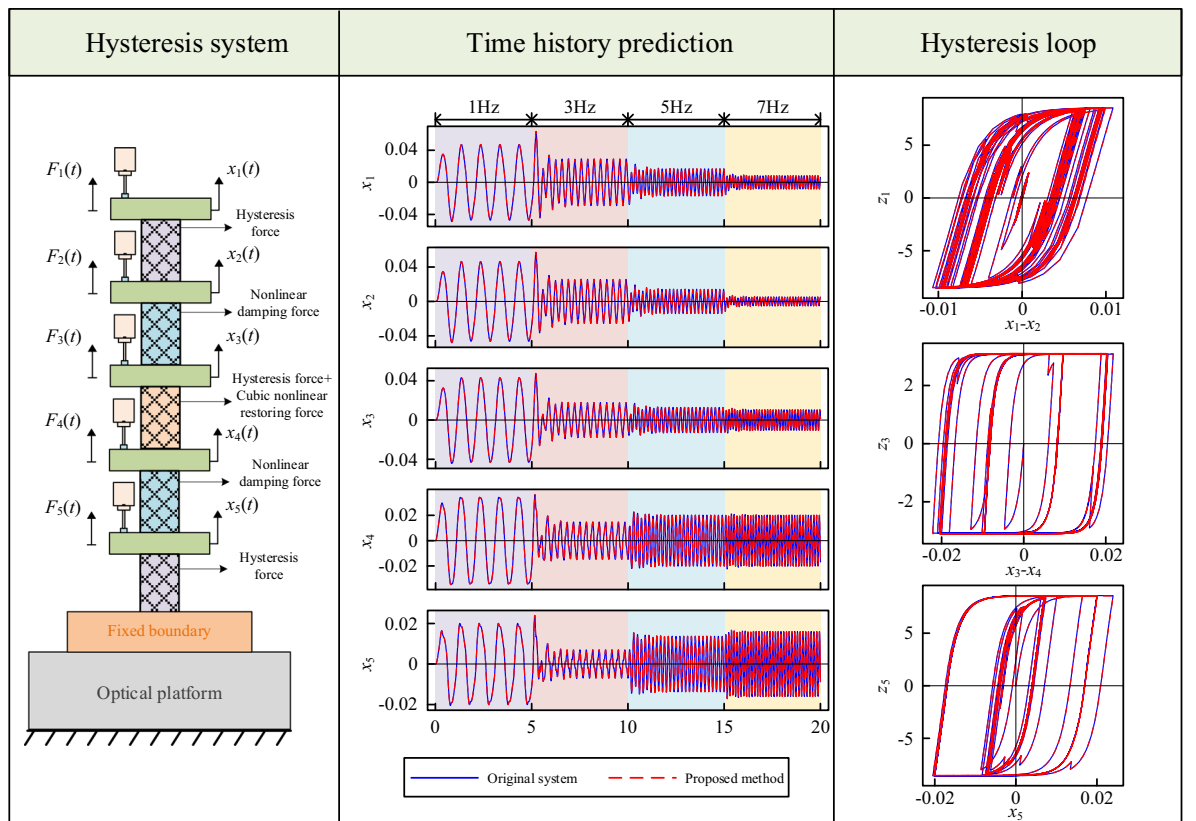


Fig. 7 Model reconstruction results for two-layer nonlinear hysteresis system



**Fig. 8** Model reconstruction results for high-dimensional nonlinear hysteresis system

of the proposed data-driven method in the discovery of multiple degrees of freedom hysteresis systems.

### 3.3.2 Multi-layers nonlinear hysteresis system

To demonstrate the capability of the proposed data-driven method to reconstruct the dynamic model of high-dimensional complex nonlinear hysteresis systems, a multi-layers nonlinear hysteresis system is studied here. The scheme diagram is shown in Fig. 8, and the corresponding governing equations are shown in Appendix 3. The candidate functions for the nonlinear restoring forces and damping forces are chosen as polynomial functions up to fifth order, the corresponding library functions in the nonlinear constitutive function library matrix  $\Theta \mathbf{n}_i$  can be obtained by Eqs. (15–18). With the proposed data-driven method, the model reconstruction results are shown Fig. 8.

It can be seen from Fig. 8 that the proposed method successfully reconstructs the governing equations of

the high-dimensional nonlinear hysteresis system. As a result, a good agreement in the time history response and hysteresis loop for excitation of different frequencies, which verifies that the proposed method is suitable for high-dimensional complex nonlinear systems.

## 4 Experiments

The above case studies come from numerical simulation with artificial noise. In this section, the experiment reconstruction of an origami structure called Tachi-Miura polyhedron (TMP) is conducted to verify the method and show its noise immunity. Since origami structures possess both geometric nonlinearity and hysteresis nonlinearity, the accurate dynamic model is difficult to be established by theoretical methods, such as Newton or Lagrange methods. Thus, the model reconstruction method proposed in this

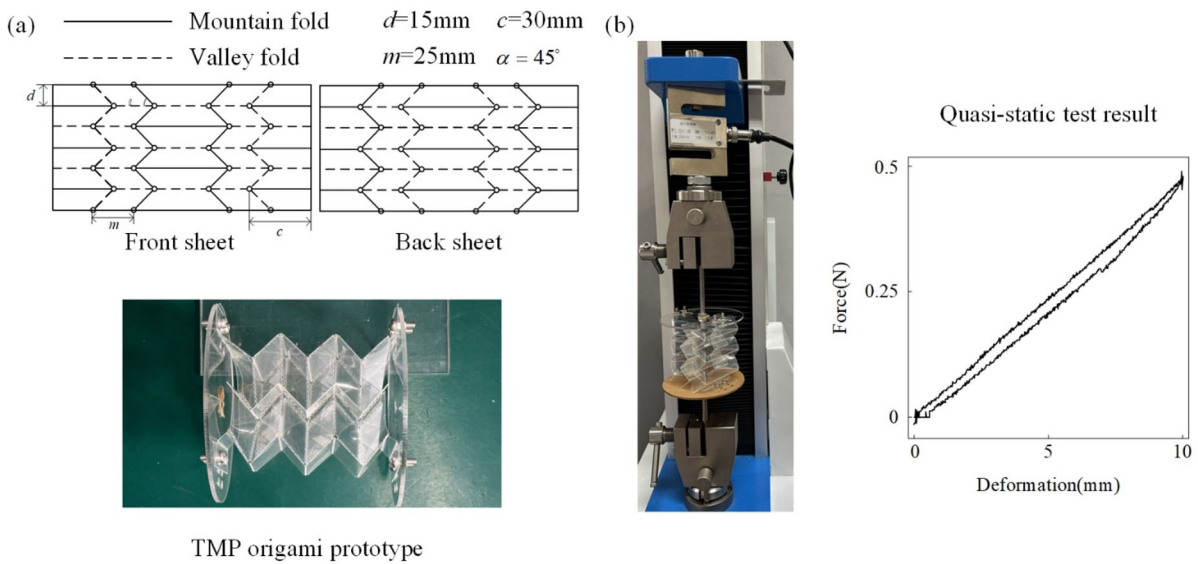


**Fig. 9** a The crease pattern of TMP and TMP experimental prototype; b Static experiment setup and constitutive relation obtained by quasi-static tests

study is applied to obtain an accurate model of TMP structure.

The crease pattern and the experimental prototype of TMP structure are shown in Fig. 9a. We use polyethylene terephthalate film (0.08 mm thickness) for the main origami body and acrylic plate (2 mm thickness) for the connection components, which are both cut by a laser cutting machine. The 2D origami patterns are folded and assembled by hand to form the TMP experimental prototype. Firstly, the quasi-static tests of the TMP structure are performed, the static experiment setup and the obtained constitutive relation are shown in Fig. 9b. It can be observed from Fig. 9b that the TMP structure shows obvious hysteresis phenomenon. However, although the constitutive relation curves of TMP structure under specific load can be obtained from the quasi-static tests, an appropriate model to describe the hysteresis constitutive relation of TMP structures under different loads cannot be obtained.

Thus, it is of great significance to reconstruct the constitutive relation and governing equations of TMP structure with both hysteresis and nonlinearity by dynamic information. The dynamic experimental setup is schematically illustrated in Fig. 10a. The experimental prototypes of the origami structures are connected to the shaker, which provide base excitation during the experiment. The excitation signal is

generated by a signal generator and transmitted to the shaker through a power amplifier. Two laser vibrometers are used to measure the displacement of the base and the free end of the origami structures separately. It should be noted that no lumped mass is attached to the free end of the TMP structure to concentrate on influence of the constitutive and inertia of the TMP structure itself on its static/dynamic behavior. The experimental reconstruction process of TMP experimental prototype is shown in Fig. 10b. First, incremental data generation of dynamics under supervision is applied to the TMP structure. In the experiment, a harmonic base excitation is first applied, which generates small amplitude response for the reconstruction of linear forces. By adjusting the frequency of the harmonic excitation to make it closer to the natural frequency of the structure, and increasing the amplitude of the basic excitation, the large amplitude response is generated for the reconstruction of nonlinear and hysteresis forces. Then, the kernel function is used to cluster the data, and the nonlinear constitutive function library matrix is constructed. Here, the candidate functions for the nonlinear restoring forces and damping forces are chosen as polynomial functions up to fourth order, the corresponding library functions in the nonlinear constitutive function library matrix  $\Theta \mathbf{n}_i$  can be obtained by Eqs. (15–18). Finally, all the nonlinear parameters are solved in the

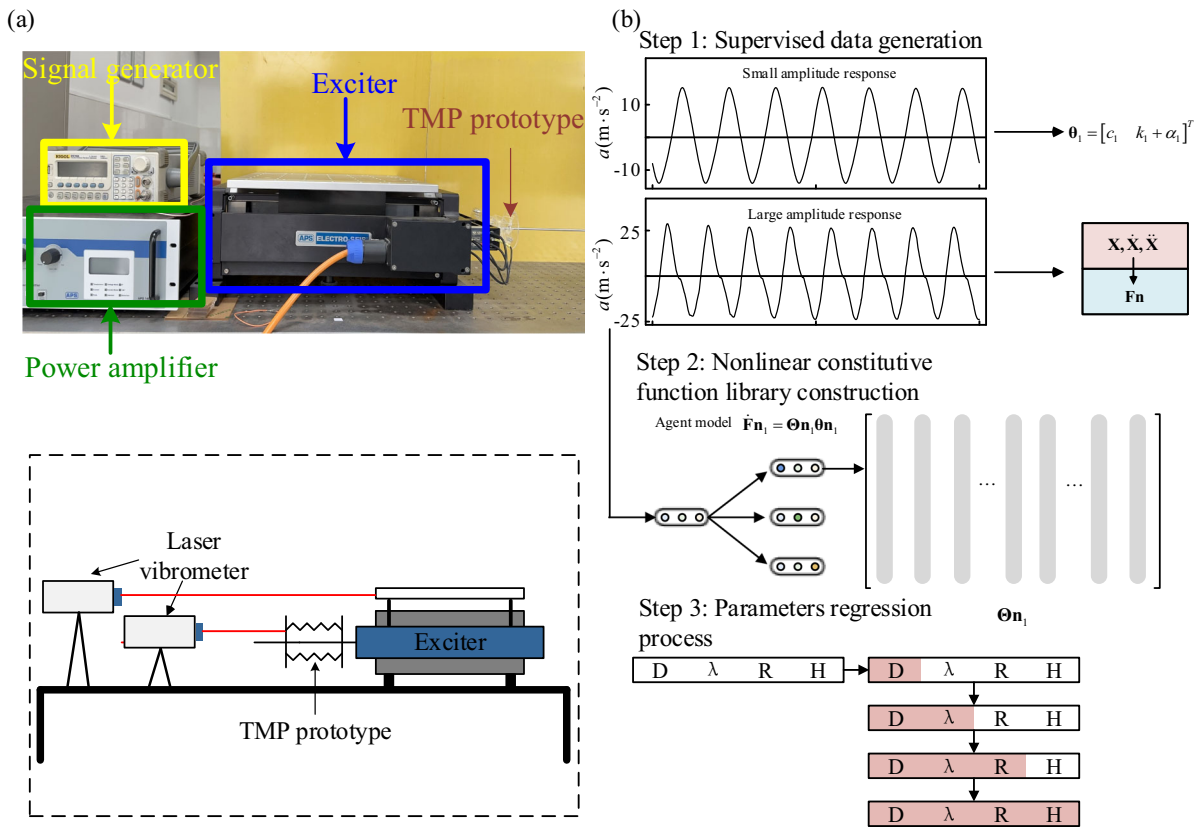


**Fig. 10** a Dynamic experimental setup; b Experimental reconstruction process of TMP experimental prototype

parameter regression process by the generalized sparse regression method. By applying the proposed data-driven method, the governing equations of the TMP origami structure can be obtained. The reconstruction results are shown in Fig. 11.

To verify the correctness of the reconstruction results, the time history prediction is conducted by comparing the experimental measured responses and the reconstruction model output under harmonic excitations with different amplitude and frequency. The output of the reconstruction model is obtained by solving the reconstructed governing equations numerically. The initial conditions in the numerical simulations are adopted as zero initial conditions. The amplitude and frequency of the base excitation are obtained using experimental data. The time history prediction results under two different harmonic excitations are shown in F. It can be seen that the time history prediction of the reconstruction model has a good agreement with the experimental measured response, which verify the correctness of the

reconstruction model, and thus demonstrate the effectiveness of the proposed data-driven model reconstruction method. Based on the reconstruction model of TMP structure, the hysteresis loops under different harmonic excitations are also shown in Fig. 11. It can be seen that hysteresis loops change with the frequency and amplitude of external excitations, which is consistent with the rate-dependent characteristics of hysteresis phenomenon. A large response results in an increase in the area enclosed by the hysteresis loop.

### 5 Conclusions

A data-driven model reconstruction method for the nonlinear hysteresis systems with different degrees of freedom is proposed based on perception of dynamics, which takes both hysteresis forces and other explicitly expressed nonlinear forces into account. The proposed data-driven method is verified by numerical

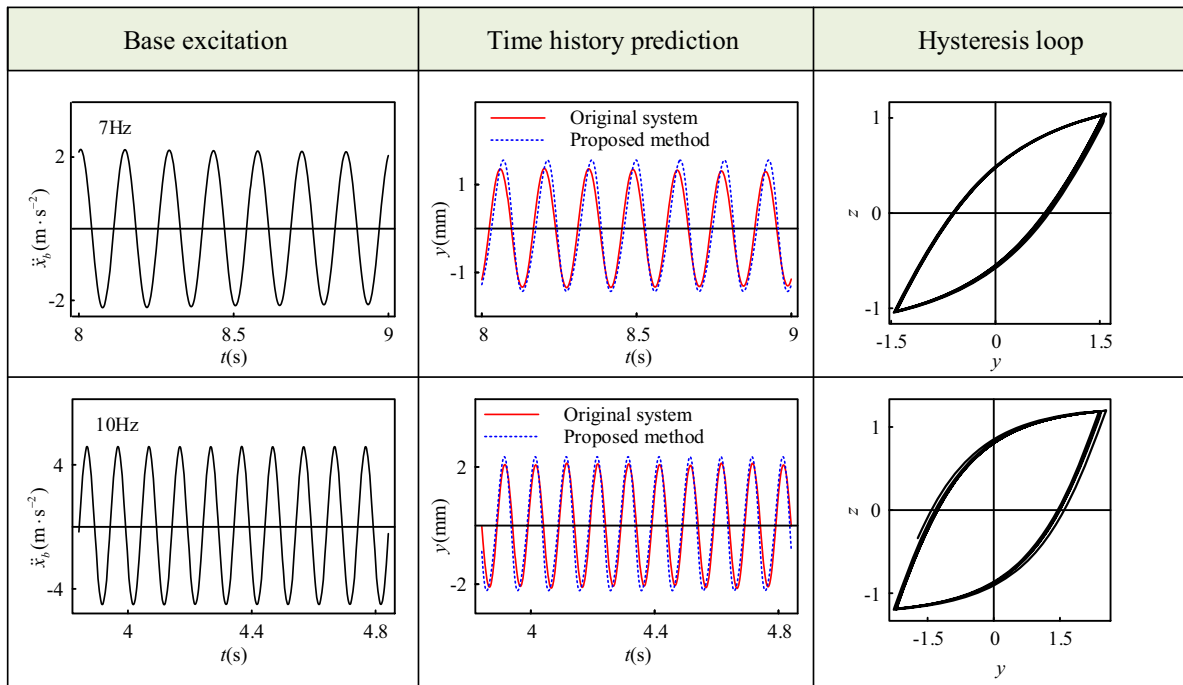


**Fig. 11** Model reconstruction results for TMP origami structure

simulations and experiment. The main contributions of this paper are summarized as follows.

1. The proposed data-driven model reconstruction method can reconstruct the constitutive relationships and governing equations of the hysteresis systems by dynamic information. Without making the assumption that only hysteresis nonlinearity exists in the hysteresis system, both hysteresis forces and other explicitly expressed nonlinear forces can be reconstructed.
2. In the proposed method, the linear and nonlinear forces are separately reconstructed by incremental data generation of dynamics under supervision. Then, based on the agent model, the nonlinear constitutive function library matrix is constructed to form the regression problem for the reconstruction of nonlinear forces. The regression problem is then solved by the generalized sparse regression method for the sparsity and accuracy of reconstruction model.
3. According to the results of the three numerical examples, the effectiveness of the proposed data-driven model reconstruction method is verified and its capability of handling hysteresis systems

with multiple degrees of freedom and different hysteresis model is demonstrated.

4. The experiment results show that demonstrate the proposed data-driven model reconstruction method could be applied to the experimental model reconstruction of hysteresis structures, which further demonstrates the effectiveness and capability of the proposed method.

The proposed method makes fully use of dynamic information of the nonlinear hysteresis nonlinear systems, which enables the method have good generalization ability, and can accurately describe the dynamics of the system under different excitation amplitudes and frequencies. Besides, the form of geometric, hysteresis and constitutive nonlinearity are separately and explicitly obtained, which makes the reconstruction model rather interpretable. This is helpful for dynamic analysis and control of hysteresis nonlinear systems. However, the main disadvantage of the proposed method is that it is only suitable differential-based hysteresis models not operator-based hysteresis models. It is worth investigating how to extend the method to operator-based hysteresis models. In conclusion, the proposed data-driven method

can deal with the model reconstruction problem of nonlinear hysteresis system with both hysteresis force and explicitly expressed nonlinear forces. Therefore, the proposed data-driven method has significant potential applications in the fields of robotics, vibration isolation, deployable structures, etc.

**Acknowledgements** The authors would like to gratefully acknowledge the support from National Natural Science Foundation of China under Grants 12122208, 12372043, 11932015, Research Grant Council of the Hong Kong SAR (PolyU 152023/20E) and Fundamental Research Funds for Central Universities. L. Cheng acknowledges the support from the Research Research Institute for Artificial Intelligence of Things (RIAIoT) of the Hong Kong Polytechnic University through project P0049625.

**Author contributions** JQ: conceptualization, methodology, software, validation, formal analysis, investigation, data acuration, visualization, writing—original draft. XS: conceptualization, methodology, funding acquisition, supervision, writing—review and editing. JX: conceptualization, funding acquisition, supervision. LC: funding acquisition, supervision.

**Data availability** All data generated or analyzed during this study are included in this published article.

**Declarations**

**Conflict of interest** The authors have not disclosed any competing interests.

**Appendix 1 Expression of linear function library matrix and corresponding linear parameters**

The expression of linear function library matrix is

$$\Theta_1(\mathbf{x}, \dot{\mathbf{x}}, \ddot{\mathbf{x}}, \mathbf{u}) = \begin{bmatrix} \mid & \mid & \mid \\ \dot{x}_2 - \dot{x}_1 & x_2 - x_1 & u_1 \\ \mid & \mid & \mid \end{bmatrix}, \quad (\text{A.1})$$

$$\Theta_i(\mathbf{x}, \dot{\mathbf{x}}, \ddot{\mathbf{x}}, \mathbf{u}) = \begin{bmatrix} \mid & \mid & \mid & \mid & \mid & \mid \\ -\ddot{x}_1 & \cdots & -\ddot{x}_{i-1} & -\dot{y}_i & -y_i & u_1 + \cdots + u_i \\ \mid & \mid & \mid & \mid & \mid & \mid \end{bmatrix},$$

$i = 2, \dots, n.$

(A.2)

where the corresponding linear parameters are

$$\theta_1 = \begin{bmatrix} c_1 & \frac{k_1 + \alpha_1}{m_1} & \frac{1}{m_1} \end{bmatrix}^T, \quad (\text{A.3})$$

$$\theta_i = \begin{bmatrix} \frac{m_1}{m_i} & \cdots & \frac{m_{i-1}}{m_i} & \frac{c_i}{m_i} & \frac{k_i + \alpha_i}{m_i} & \frac{1}{m_i} \end{bmatrix}^T. \quad (\text{A.4})$$

**Appendix 2 Nonlinear constitutive function library construction in hysteresis system with nonlinear damping force**

The nonlinear constitutive function library matrix can be expressed as

$$\Theta_{n_i}(y_i, \dot{y}_i, \mathbf{f}_i, \mathbf{F}_{n_i}) = \begin{bmatrix} \mid & \mid \\ \bar{Y}_i^2 \odot Y_i^2 & \bar{Y}_i^3 \odot Y_i^3 & \bar{Y}_i^4 \odot Y_i^4 & \bar{Y}_i^5 \odot Y_i^5 & Y_i^2 & Y_i^3 & Y_i^4 & Y_i^5 & y_i \odot \dot{y}_i & -y_i \odot \mathbf{F}_{n_i} \\ \mid & \mid \end{bmatrix}, \quad (\text{B.1})$$

where

$$\bar{Y}_i^2 \odot Y_i^2 = \begin{bmatrix} \mid & \mid & \mid \\ \dot{y}_i(y_i^2) & \dot{y}_i(y_i \dot{y}_i) & \dot{y}_i(\dot{y}_i^2) \\ \mid & \mid & \mid \end{bmatrix}, \quad (\text{B.2})$$

$$\bar{Y}_i^3 \odot Y_i^3 = \begin{bmatrix} \mid & \mid & \mid & \mid \\ \dot{y}_i(y_i^3) & \dot{y}_i(y_i^2 \dot{y}_i) & \dot{y}_i(y_i \dot{y}_i^2) & \dot{y}_i(\dot{y}_i^3) \\ \mid & \mid & \mid & \mid \end{bmatrix}, \quad (\text{B.3})$$

$$\bar{Y}_i^4 \odot Y_i^4 = \begin{bmatrix} \mid & \mid & \mid & \mid & \mid \\ \dot{y}_i(y_i^4) & \dot{y}_i(y_i^3 \dot{y}_i) & \dot{y}_i(y_i^2 \dot{y}_i^2) & \dot{y}_i(y_i \dot{y}_i^3) & \dot{y}_i(\dot{y}_i^4) \\ \mid & \mid & \mid & \mid & \mid \end{bmatrix}, \quad (\text{B.4})$$

$$\bar{Y}_i^5 \odot Y_i^5 = \begin{bmatrix} \mid & \mid & \mid & \mid & \mid & \mid \\ \dot{y}_i(y_i^5) & \dot{y}_i(y_i^4 \dot{y}_i) & \dot{y}_i(y_i^3 \dot{y}_i^2) & \dot{y}_i(y_i^2 \dot{y}_i^3) & \dot{y}_i(y_i \dot{y}_i^4) & \dot{y}_i(\dot{y}_i^5) \\ \mid & \mid & \mid & \mid & \mid & \mid \end{bmatrix}, \quad (\text{B.5})$$

$$\dot{Y}_i^2 = \begin{bmatrix} \mid & \mid \\ \frac{d(y_i \dot{y}_i)}{dt} & \frac{d(\dot{y}_i^2)}{dt} \\ \mid & \mid \end{bmatrix}, \quad (\text{B.6})$$

$$\dot{\mathbf{Y}}_i^3 = \left[ \frac{d(y_i^2 \dot{y}_i)}{dt} \quad \frac{d(y_i \dot{y}_i^2)}{dt} \quad \frac{d(\dot{y}_i^3)}{dt} \right], \tag{B.7}$$

$$\dot{\mathbf{Y}}_i^4 = \left[ \frac{d(y_i^3 \dot{y}_i)}{dt} \quad \frac{d(y_i^2 \dot{y}_i^2)}{dt} \quad \frac{d(y_i \dot{y}_i^3)}{dt} \quad \frac{d(\dot{y}_i^4)}{dt} \right], \tag{B.8}$$

$$\dot{\mathbf{Y}}_i^5 = \left[ \frac{d(y_i^4 \dot{y}_i)}{dt} \quad \frac{d(y_i^3 \dot{y}_i^2)}{dt} \quad \frac{d(y_i^2 \dot{y}_i^3)}{dt} \quad \frac{d(y_i \dot{y}_i^4)}{dt} \quad \frac{d(\dot{y}_i^5)}{dt} \right]. \tag{B.9}$$

The expression of nonlinear coefficients  $\theta \mathbf{n}_i$  is

$$\theta \mathbf{n}_i = \left[ \xi_{i2} \quad \xi_{i3} \quad \xi_{i4} \quad \xi_{i5} \quad \psi_{i2} \quad \psi_{i3} \quad \psi_{i4} \quad \psi_{i5} \quad 2a_{i1} - \frac{\lambda_i \alpha_i}{m_i} \quad \lambda_i \right]^T, \tag{B.10}$$

$$\xi_{i2} = [\lambda_i a_{i1} + 3a_{i4} \quad \lambda_i a_{i2} \quad \lambda_i a_{i3}], \tag{B.11}$$

$$\xi_{i3} = [\lambda_i a_{i4} + 4a_{i8} \quad \lambda_i a_{i5} \quad \lambda_i a_{i6} \quad \lambda_i a_{i7}], \tag{B.12}$$

$$\xi_{i4} = [\lambda_i a_{i8} + 5a_{i13} \quad \lambda_i a_{i9} \quad \lambda_i a_{i10} \quad \lambda_i a_{i11} \quad \lambda_i a_{i12}], \tag{B.13}$$

$$\xi_{i5} = [\lambda_i a_{i13} \quad \lambda_i a_{i14} \quad \lambda_i a_{i15} \quad \lambda_i a_{i16} \quad \lambda_i a_{i17} \quad \lambda_i a_{i18}], \tag{B.14}$$

$$\psi_{i2} = [a_{i2} \quad a_{i3}], \tag{B.15}$$

$$\psi_{i3} = [a_{i5} \quad a_{i6} \quad a_{i7}], \tag{B.16}$$

$$\psi_{i4} = [a_{i9} \quad a_{i10} \quad a_{i11} \quad a_{i12}], \tag{B.17}$$

$$\psi_{i5} = [a_{i14} \quad a_{i15} \quad a_{i16} \quad a_{i17} \quad a_{i18}]. \tag{B.18}$$

### Appendix 3 Governing equations of multi-layers nonlinear hysteresis system

The governing equations of the multi-layers nonlinear hysteresis system are

$$\mathbf{M}\ddot{\mathbf{x}} + \mathbf{C}\dot{\mathbf{x}} + \mathbf{K}\mathbf{x} + \mathbf{g}_n(\mathbf{x}, \dot{\mathbf{x}}) + \mathbf{z}(\mathbf{x}, \dot{\mathbf{x}}) = \mathbf{F}(t), \tag{C.1}$$

where

$$\mathbf{M} = \begin{bmatrix} m_1 & 0 & 0 & 0 & 0 \\ 0 & m_2 & 0 & 0 & 0 \\ 0 & 0 & m_3 & 0 & 0 \\ 0 & 0 & 0 & m_4 & 0 \\ 0 & 0 & 0 & 0 & m_5 \end{bmatrix}, \tag{C.2}$$

$$\mathbf{C} = \begin{bmatrix} c_1 & -c_1 & 0 & 0 & 0 \\ -c_1 & c_1 + c_2 & -c_2 & 0 & 0 \\ 0 & -c_2 & c_2 + c_3 & -c_3 & 0 \\ 0 & 0 & -c_3 & c_3 + c_4 & -c_4 \\ 0 & 0 & 0 & -c_4 & c_4 + c_5 \end{bmatrix}, \tag{C.3}$$

$$\mathbf{K} = \begin{bmatrix} k_1 & -k_1 & 0 & 0 & 0 \\ -k_1 & k_1 + k_2 & -k_2 & 0 & 0 \\ 0 & -k_2 & k_2 + k_3 & -k_3 & 0 \\ 0 & 0 & -k_3 & k_3 + k_4 & -k_4 \\ 0 & 0 & 0 & -k_4 & k_4 + k_5 \end{bmatrix}, \tag{C.4}$$

$$\mathbf{g}_n(\mathbf{x}, \dot{\mathbf{x}}) = \begin{bmatrix} 0 \\ c_{23}(x_2 - x_3)^2(\dot{x}_2 - \dot{x}_3) \\ -c_{23}(x_2 - x_3)^2(\dot{x}_2 - \dot{x}_3) + k_{33}(x_3 - x_4)^3 \\ -k_{33}(x_3 - x_4)^3 + c_{43}(x_4 - x_5)^2(\dot{x}_4 - \dot{x}_5) \\ -c_{43}(x_4 - x_5)^2(\dot{x}_4 - \dot{x}_5) \end{bmatrix}, \tag{C.5}$$

$$\mathbf{z}(\mathbf{x}, \dot{\mathbf{x}}) = \begin{bmatrix} z_1 \\ -z_3 \\ z_3 \\ -z_5 \\ z_5 \end{bmatrix}. \tag{C.6}$$

$$\begin{aligned} \dot{z}_1 &= \alpha_1(\dot{x}_1 - \dot{x}_2) - \gamma_1|\dot{x}_1 - \dot{x}_2|z_1 - \delta_1(\dot{x}_1 - \dot{x}_2)|z_1|, \\ \dot{z}_3 &= \alpha_3(\dot{x}_3 - \dot{x}_4) - \gamma_3|\dot{x}_3 - \dot{x}_4|z_3 - \delta_3(\dot{x}_3 - \dot{x}_4)|z_3|, \\ \dot{z}_5 &= \alpha_5\dot{x}_5 - \gamma_5|\dot{x}_5|z_5 - \delta_5\dot{x}_5|z_5|. \end{aligned} \tag{C.7}$$

### References

1. Wang, L., Guo, J., Takewaki, I.: Real-time hysteresis identification in structures based on restoring force reconstruction and Kalman filter. *Mech. Syst. Signal Proc.* **150**, 107297 (2021)
2. Ismail, M., Ikhouane, F., Rodellar, J.: The hysteresis Bouc-Wen model, a survey. *Arch. Comput. Method Eng.* **16**(2), 161–188 (2009)
3. Fan, Y., He, X., Zhang, F., et al.: Fano-resonant hybrid metamaterial for enhanced nonlinear tunability and hysteresis behavior. *Research* **2021**, 9754083 (2021)

4. Hu, K., Jeannin, T., Berre, J., et al.: Toward actuation of Kresling pattern-based origami robots. *Smart Mater. Struct.* **31**(10), 105025 (2022)
5. Nayakanti, N., Tawfik, S.H., Hart, A.J.: Twist-coupled Kirigami cells and mechanisms. *Extreme Mech. Lett.* **21**, 17–24 (2018)
6. Rossi, N., Méndez, C.G., Huespe, A.E.: Surrogate model for a mechanical metamaterial undergoing microstructure instabilities and phase transformations. *Int. J. Mech. Sci.* **243**, 107913 (2023)
7. Sun, S., An, N., Wang, G., et al.: Snap-back induced hysteresis in an elastic mechanical metamaterial under tension. *Appl. Phys. Lett.* **115**(9), 091901 (2019)
8. Zhou, Y., Zhang, Q., Cai, J.G., et al.: Experimental study of the hysteretic behavior of energy dissipation braces based on Miura origami. *Thin-Walled Struct.* **167**, 10 (2021)
9. Chen, Y., Kang, G., Yuan, J., et al.: An electro-mechanically coupled visco-hyperelastic-plastic constitutive model for cyclic deformation of dielectric elastomers. *Mech. Mater.* **150**, 103575 (2020)
10. Gu, G.Y., Zhu, L.M., Su, C.Y.: Modeling and compensation of asymmetric hysteresis nonlinearity for piezoceramic actuators with a modified prandtl-ishlinskii model. *IEEE Trans. Ind. Electron.* **61**(3), 1583–1595 (2014)
11. He, Y.J., Sun, Q.P.: On non-monotonic rate dependence of stress hysteresis of superelastic shape memory alloy bars. *Int. J. Solids Struct.* **48**(11–12), 1688–1695 (2011)
12. Ji, D.H., Koo, J.H., Yoo, W.J., et al.: Precise tracking control of piezoelectric actuators based on a hysteresis observer. *Nonlinear Dyn.* **70**(3), 1969–1976 (2012)
13. Lin, J., Zheng, S.Y., Xiao, R., et al.: Constitutive behaviors of tough physical hydrogels with dynamic metal-coordinated bonds. *J. Mech. Phys. Solids* **139**, 13 (2020)
14. Qi, Z., Sun, X.: The modular gait design of a soft, earthworm-like locomotion robot driven by ultra-low frequency excitation. *Appl. Sci.-Basel.* **13**(4), 2723 (2023)
15. Stupkiewicz, S., Rezaee-Hajidehi, M., Petryk, H.: Multiscale analysis of the effect of interfacial energy on non-monotonic stress–strain response in shape memory alloys. *Int. J. Solids Struct.* **221**, 77–91 (2021)
16. Zhong, D.M., Xiang, Y.H., Wang, Z.C., et al.: A visco-hyperelastic model for hydrogels with tunable water content. *J. Mech. Phys. Solids* **173**, 21 (2023)
17. Bhovad, P., Kaufmann, J., Li, S.Y.: Peristaltic locomotion without digital controllers: exploiting multi-stability in origami to coordinate robotic motion. *Extreme Mech. Lett.* **32**, 100552 (2019)
18. Sadeghi, S., Allison, S.R., Bestill, B., et al.: TMP origami jumping mechanism with nonlinear stiffness. *Smart Mater. Struct.* **30**(6), 14 (2021)
19. Misseroni, D., Pratapa, P.P., Liu, K., et al.: Experimental realization of tunable Poisson’s ratio in deployable origami metamaterials. *Extreme Mech. Lett.* **53**, 10 (2022)
20. Yasuda, H., Yang, J.: Reentrant origami-based metamaterials with negative poisson’s ratio and bistability. *Phys. Rev. Lett.* **114**(18), 5 (2015)
21. Gillman, A., Fuchi, K., Buskohl, P.R.: Truss-based nonlinear mechanical analysis for origami structures exhibiting bifurcation and limit point instabilities. *Int. J. Solids Struct.* **147**, 80–93 (2018)
22. Sun, X.H., Wu, S., Dai, J.Z., et al.: Phase diagram and mechanics of snap-folding of ring origami by twisting. *Int. J. Solids Struct.* **248**, 21 (2022)
23. Ha, C.S., Lakes, R.S., Plesha, M.E.: Cubic negative stiffness lattice structure for energy absorption: numerical and experimental studies. *Int. J. Solids Struct.* **178**, 127–135 (2019)
24. Jiang, D.J., Bechle, N.J., Landis, C.M., et al.: Buckling and recovery of NiTi tubes under axial compression. *Int. J. Solids Struct.* **80**, 52–63 (2016)
25. Rao, A., Ruimi, A., Srinivasa, A.R.: Internal loops in superelastic shape memory alloy wires under torsion - Experiments and simulations/predictions. *Int. J. Solids Struct.* **51**(25–26), 4554–4571 (2014)
26. Woodworth, L.A., Lohse, F., Kopelmann, K., et al.: Development of a constitutive model considering functional fatigue and pre-stretch in shape memory alloy wires. *Int. J. Solids Struct.* **234**, 16 (2022)
27. Xiao, Y., Jiang, D.J.: Effects of structural geometry on the localized deformation of superelastic NiTi sheets. *Int. J. Solids Struct.* **257**, 17 (2022)
28. Li, Z., Shan, J.J., Gabbert, U.: Inverse compensation of hysteresis using krasnoselskii-pokrovskii model. *IEEE-ASME Trans. Mechatron.* **23**(2), 966–971 (2018)
29. Liu, Y.F., She, J.Y., Duan, H.Y., et al.: Hybrid model based on maxwell-slip model and relevance vector machine. *IEEE Trans. Ind. Electron.* **68**(10), 10050–10057 (2021)
30. Yi, S.C., Yang, B.T., Meng, G.: Microvibration isolation by adaptive feedforward control with asymmetric hysteresis compensation. *Mech. Syst. Signal Proc.* **114**, 644–657 (2019)
31. Zhang, J., Torres, D., Sepulveda, N., et al.: A compressive sensing-based approach for Preisach hysteresis model identification. *Smart Mater. Struct.* **25**(7), 12 (2016)
32. Wang, X.J., Alici, G., Tan, X.B.: Modeling and inverse feedforward control for conducting polymer actuators with hysteresis. *Smart Mater. Struct.* **23**(2), 9 (2014)
33. Zhu, H.T., Rui, X.T., Yang, F.F., et al.: An efficient parameters identification method of normalized Bouc-Wen model for MR damper. *J. Sound Vib.* **448**, 146–158 (2019)
34. Ye, M.Y., Wang, X.D.: Parameter estimation of the Bouc-Wen hysteresis model using particle swarm optimization. *Smart Mater. Struct.* **16**(6), 2341–2349 (2007)
35. Quaranta, G., Lacarbonara, W., Masri, S.F.: A review on computational intelligence for identification of nonlinear dynamical systems. *Nonlinear Dyn.* **99**(2), 1709–1761 (2020)
36. Masri, S.F., Chassiakos, A.G., Caughey, T.K.: Identification of nonlinear dynamic systems using neural networks. *J. Appl. Mech.* **60**(1), 123–133 (1993)
37. Agarwal, V., Wang, R., Balachandran, B.: Data driven forecasting of aperiodic motions of non-autonomous systems. *Chaos* **31**(2), 021105 (2021)
38. Wang, R., Kalnay, E., Balachandran, B.: Neural machine-based forecasting of chaotic dynamics. *Nonlinear Dyn.* **98**(4), 2903–2917 (2019)
39. Serpico, C., Visone, C.: Magnetic hysteresis modeling via feed-forward neural networks. *IEEE Trans. Magn.* **34**(3), 623–628 (1998)

40. Zakerzadeh, M.R., Naseri, S.: Modelling hysteresis in shape memory alloys using LSTM recurrent neural network. *J. Appl. Math.* **2024**, 1174438 (2024)
41. Kyprianou, A., Worden, K., Panet, M.: Identification of hysteretic systems using the differential evolution algorithm. *J. Sound Vib.* **248**(2), 289–314 (2001)
42. Zhang, H.C., Foliente, G.C., Yang, Y.M., et al.: Parameter identification of inelastic structures under dynamic loads. *Earthq. Eng. Struct. Dyn.* **31**(5), 1113–1130 (2002)
43. Li, Z.J., Shu, G.P.: Hysteresis characterization and identification of the normalized Bouc-Wen model. *Struct. Eng. Mech.* **70**(2), 209–219 (2019)
44. Charalampakis, A.E., Dimou, C.K.: Identification of bouc-wen hysteretic systems using particle swarm optimization. *Comput. Struct.* **88**(21–22), 1197–1205 (2010)
45. Worden, K., Manson, G.: On the identification of hysteretic systems. Part I: Fitness landscapes and evolutionary identification. *Mech. Syst. Signal Proc.* **29**, 201–212 (2012)
46. Carboni, B., Lacarbonara, W., Brewick, P.T., et al.: Dynamical response identification of a class of nonlinear hysteretic systems. *J. Intell. Mater. Syst. Struct.* **29**(13), 2795–2810 (2018)
47. Ortiz, G.A., Alvarez, D.A., Bedoya-Ruiz, D.: Identification of bouc-wen type models using multi-objective optimization algorithms. *Comput. Struct.* **114**, 121–132 (2013)
48. Lin, M., Sun, B., Cheng, C., et al.: Alternating state-parameter identification of Bouc-Wen hysteretic systems from steady-state harmonic response. *J. Sound Vib.* **538**, 117242 (2022)
49. Lin, M., Cheng, C., Zhang, G., et al.: Identification of Bouc-Wen hysteretic systems based on a joint optimization approach. *Mech. Syst. Signal Proc.* **180**, 109404 (2022)
50. Li, D., Wang, Y.: Parameter identification of a differentiable bouc-wen model using constrained extended kalman filter. *Struct. Control Hlth.* **20**(1), 360–378 (2021)
51. Niola, V., Palli, G., Strano, S., et al.: Nonlinear estimation of the bouc-wen model with parameter boundaries: application to seismic isolators. *Comput. Struct.* **222**, 1–9 (2019)
52. Calabrese, A., Strano, S., Terzo, M.: Adaptive constrained unscented Kalman filtering for real-time nonlinear structural system identification. *Struct. Control Hlth.* **25**(2), e2084 (2018)
53. Ojha, S., Kalimullah, N.M.M., Shelke, A.: Application of constrained unscented Kalman filter (CUKF) for system identification of coupled hysteresis under bidirectional excitation. *Struct. Control Hlth.* **29**(12), e3115 (2022)
54. Li, S.J., Suzuki, Y., Noori, M.: Identification of hysteretic systems with slip using bootstrap filter. *Mech. Syst. Signal Proc.* **18**(4), 781–795 (2004)
55. Brunton, S.L., Proctor, J.L., Kutz, J.N.: Discovering governing equations from data by sparse identification of nonlinear dynamical systems. *Proc. Natl. Acad. Sci. U. S. A.* **113**(15), 3932–3937 (2016)
56. Rudy, S.H., Brunton, S.L., Proctor, J.L., et al.: Data-driven discovery of partial differential equations. *Sci. Adv.* **3**(4), 6 (2017)
57. Guan, Y.F., Brunton, S.L., Novosselov, I.: Sparse nonlinear models of chaotic electroconvection. *R. Soc. Open Sci.* **8**(8), 13 (2021)
58. Kaptanoglu, A.A., Callaham, J.L., Aravkin, A., et al.: Promoting global stability in data-driven models of quadratic nonlinear dynamics. *Phys. Rev. Fluids.* **6**(9), 30 (2021)
59. Mendible, A., Koch, J., Lange, H., et al.: Data-driven modeling of rotating detonation waves. *Phys. Rev. Fluids.* **6**(5), 20 (2021)
60. Messenger, D.A., Bortz, D.M.: Weak SINDy for partial differential equations. *J. Comput. Phys.* **443**, 27 (2021)
61. Messenger, D.A., Bortz, D.M.: Weak SINDy: galerkin-based data-driven model selection. *Multiscale Model. Simul.* **19**(3), 1474–1497 (2021)
62. Messenger, D.A., Bortz, D.M.: Learning mean-field equations from particle data using WSINDy. *Phys. D* **439**, 18 (2022)
63. Qian, J.W., Sun, X.T., Xu, J.: A data-driven reconstruction method for dynamic systems with multistable property. *Nonlinear Dyn.* **111**(5), 4517–4541 (2023)
64. Sun, X.T., Qian, J.W., Xu, J.: Compressive-sensing model reconstruction of nonlinear systems with multiple attractors. *Int. J. Mech. Sci.* **265**, 108905 (2024)

**Publisher's Note** Springer Nature remains neutral with regard to jurisdictional claims in published maps and institutional affiliations.

Springer Nature or its licensor (e.g. a society or other partner) holds exclusive rights to this article under a publishing agreement with the author(s) or other rightsholder(s); author self-archiving of the accepted manuscript version of this article is solely governed by the terms of such publishing agreement and applicable law.